

# Performance Analysis of Grid Integrated Doubly Fed Induction Generator for a Small Hydropower Plant

Sanjeev Kumar Gagrai\*, Sundram Mishra\*\*<sup>‡</sup>, Madhu Singh\*\*\*

\*Department of Electrical and Electronics Engineering, NIT, Jamshedpur (831014), Jharkhand, India

\*\* Department of Electrical and Electronics Engineering, NIT, Jamshedpur (831014), Jharkhand, India

\*\*\* Department of Electrical and Electronics Engineering, NIT, Jamshedpur (831014), Jharkhand, India

(Sanjeev.mit03@gmail.com, sundram79808183@gmail.com, madhu.ee@nitjsr.ac.in)

<sup>‡</sup>Corresponding Author; Sundram Mishra, Department of Electrical and Electronics Engineering, NIT, Jamshedpur (831014), Jharkhand, India, Tel: 9354701980, sundram79808183@gmail.com

*Received: 23.08.2018 Accepted:21.09.2018*

**Abstract-** The motive of this work is to present the modeling and simulation of a hydraulic turbine which is driven by a doubly-fed induction generator and the generated ac power given to the grid. For feeding the ac power to the grid, we are using two PWM voltage source converters which are connected back to back between the utility grid and rotor terminals with the help of a common dc-link. Machine side converter is used for pertinent excitation. The power flow between AC side and DC bus is controlled by a grid side converter (GSC) which also allows the system to be operated in less than and greater than synchronous speed mode of operation. MATLAB/SIMULINK is used for Time domain simulations. The system is stable under different load conditions and it is investigated with the help of model and simulations result. To preserve the system stability whenever the power demand is precipitously increasing in the utility grid side, doubly fed induction generator(DFIG) system and Proportional integral(PI) controller is used.

**Keywords** Doublyfed induction generator (DFIG),Grid side converter(GSC), Rotor side converter(RSC),Utility grid.

## Nomenclature

$P_m$	Mechanical output power
$\omega_r$	Speed of Rotor in electrical
$T_m$	Input mechanical torque
$P_{hydro}$	Available hydro power
$Q$	Water discharge
$H$	Available water head
$\rho$	Water Density
$P_{out}$	Turbine Output power
$C$	Capacitance
$M_{dr}$	d-axis modulation indexes of RSC
$M_{qr}$	q-axis modulation indexes of RSC
$M_{df}$	d-axis modulation indexes of GSC
$M_{qf}$	q-axis modulation indexes of GSC
$K_{dc}$	PI-controller for DC link voltage control

### 1. Introduction

In the present era, electricity is considered as one of the rudimentary necessities for all of us now, especially in remote areas as well as it also helps to improve the affluence, urbanization and Economic growth [1, 2]. According to the ministry of renewable energy in India, the remaining 18500 odd un-electrified villages in the country would be electrified within the next 1000 days. In the present scenario, India has 249,448 MW total installed power generation capacity, although, according to Government’s guesstimate country would need nearly 800 GW of installed capacity by 2031-32 [3]. To fulfill the future growing energy demand, India needs every available source of energy [1]. In India, the renewable energy sector plays an indispensable part of the solution to encounter the nation’s energy needs. Renewable energy has been a visible impact in the Indian energy consequence throughout the past few years as India is on its mode to attaining the 175 GW target for installed renewable energy by 2022. Ministry of New and Renewable Energy(MNRE) has occupied sundry gaits for an unpolluted energy future by taking up the largest renewable capacity enlargement programme in all the world [4]. For achieving the mark of 175 GW by 2022, the generation of electricity from the small hydroelectric plant is very important and therefore, In India small hydropower plant is used as an alternative source of energy to meet the electricity demand. The thermal power plant is a most prevailing power plant in India because 60% of the total installed capacity is generated by using coal as shown in the “figure 1” [5]. India is enriched with hydropower potential and due to this, attained 5<sup>th</sup> in the world. For bucolic electrifying over the epoch of the system, small hydropower sector is the low-priced technology. Hydropower plant taking an inaugurated sufficiency of 0.025 GW is deliberated as small hydropower plant. [3]. MNRE and government of India are providing financial help and subsidy to develop the small hydropower plant sector. For industrialization and sustainable development, small hydropower plant plays a vivacious role [6].

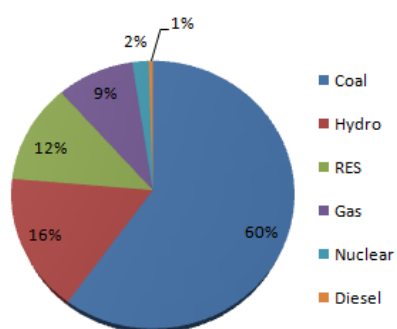


Fig.1. Pictorial representation of different sources of energy

Small hydropower plant is beneficial to the environment as well as it also helps in sustaining reduced use of fossil fuels [3, 6]. Small hydropower plant is free from resettlement, deforestation, and construction of dams as large hydropower plant is associated with these problems. Small hydropower plant(SHPP) is very much pertinent for generation of electricity in remote and secluded areas as well as having long expedient life and inflation free generation cost [2]. The pros which are given in above makes the small hydropower plant more eye-catching. In the current era, advanced power

electronics is growing undoubtedly, so the hydroelectric plant which embrace the power electronics converter and apposite regulation setup implements admirable performance like controllability of real and reactive power as well as voltage and frequency [7]. It also assists in the controllability of short circuit and fault circumstances [7]. Traditionally hydroelectric plant is associated with synchronous generator and the reason behind this is the constant output but after coming of DFIG in the fashion with adjustable power conditioner provides the copiously controllability of the system with less power rating [8, 9]. There is numerous amount of pros about the DFIG which makes the DFIG more agreeable. DFIG comprises the self-starting nature as well as blessed with three phase AC supply for excitation view [10]. It remarkably subjected to on the power electronics converter and runs in the all manners of speed like sub synchronous, synchronous and super synchronous as well as it generates the power from both rotor and stator circuit under the condition of greater than synchronous speed along with power generation is also possible in all three modes of speed. In DFIG rating of the converter is decided by the slip and this aspect makes the converter moderately rated [11]. As it is partial rated power converters due to this its installation budget is less.

### 2. Description of Hydro Energy Conversion System

Water is present in plentiful amounts in India so it is the leading source for electricity generation. Hydropower delineates the norm of water assets towards inflation free green energy in the absence of combustible charge with grown technology peculiarized by maximum prime moving efficiency and remarkable running flexibility [12,13]. Small hydropower plant associated with DFIG and back to back converter as shown in “figure2” [14].

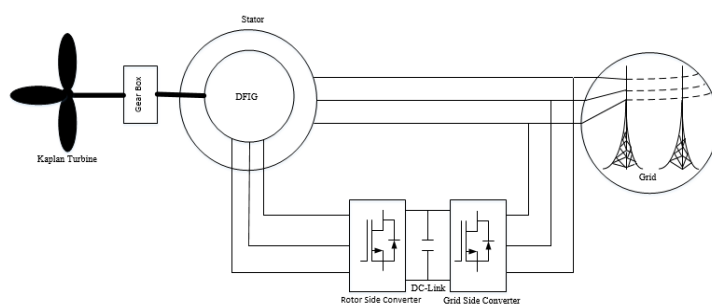


Fig.2. The arrangement of power converters with DFIG in SHPP system

For the generation of electricity from a hydroelectric plant, turbine rotation is required which is done by stored and captured energy of water to run the generator [15]. Hydropower can be categorized into three main types like as large hydropower, medium hydropower, and small hydropower. Hydropower plants are distinguished with respect to the power generation capacity as [16]:

1. Large hydropower >100MW
2. Medium hydropower >30-100MW
3. Small hydropower >2-25MW

Apart from large and medium hydropower plant, there are some additional types of a hydropower plants available to fulfill the small-scale purposes [17]. They are Pico hydropower plant ranging up to 5 kW, micro hydro plant ranging up to 100 kW, mini hydropower plant whose capacity lies between 101 kW to 2000 kW and small hydropower plant

ranging up to 2 MW to 25 MW [3]. In India most of the remote areas are not associated with grid connection. So for providing electricity to that types of areas, Pico and micro hydropower plants are used [18, 19].

3.1. Modeling of the Kaplan Turbine

For high discharge and low head power purpose, Kaplan turbine is best suited and the efficiency of this turbine is about

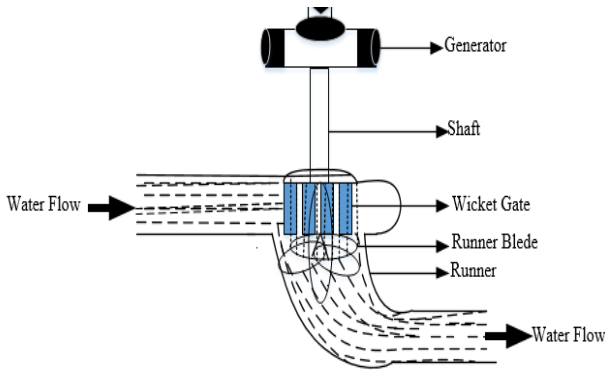


Fig. 3. Structural view of Kaplan turbine with axial water flow

The prime motive of nominating Kaplan turbine is that small hydropower plant is deliberated a run-of-river likewise most of the plants [13]. This reason motivates to the use of Kaplan turbine for hydraulic power plant and the configuration of this turbine is like a boat propeller and it is also considered as turbomachine. It is the most apposite for the low head [20]. Small hydropower plant comes under the low head (less than 10m) configuration. The water flow rate in the Kaplan turbine is guarded by wavering the slant of the wicket gate according to our prerequisite. The structural view of the Kaplan turbine is given in “figure3”. For Kaplan turbine, the torque and speed calculations are presented here. Hydropower is directly proportional to the water head and flow rate as shown in “Eq. (1)”.

$$P_{hydro} = \rho \cdot g \cdot Q \cdot H \tag{1}$$

$$P_{out} = P_m = \eta_t P_{hydro} \tag{2}$$

For utmost of the cases the efficiency of the Kaplan turbine is close to 90%. So for convenience here we are assuming 90% efficiency. The velocity of the water in penstock is

$$U = K_u G \sqrt{H} \tag{3}$$

The flow in a pipe is given as:

$$Q = AU \tag{4}$$

As torque is proportionate to the power so we can obtain torque from the developed power i.e.

$$T_m = \frac{P_{out}}{\omega} = \frac{P_m}{\omega} \tag{5}$$

Now, switching the value of  $P_{out}$  in the “Eq. (5)”

3. Modeling of the Small Hydropower Plant

to 90% or higher. Kaplan turbine is linked with a gear box and the reason of this configuration is that the speed of rotation is small. The structural view is given below [20].

$$T_m = \frac{\eta_t P_{hydro}}{\omega} \tag{6}$$

Again, switching the value of  $P_{hydro}$  in “Eq. (6)”, it develops

$$T_m = \frac{\eta_t \rho g Q H}{\omega} \tag{7}$$

When placing the value of  $Q=A.U$  in the “Eq. (7)”, it becomes as

$$T_m = \frac{\eta_t \rho g A U H}{\omega} \tag{8}$$

The mechanical torque ( $T_m$ ) depends upon the discharge of water and water head and as well as the velocity of water.

The electromagnetic equation of the system is given in “Eq. (9)”, where  $d$  denotes viscous friction coefficient.

$$J \frac{d}{dt}(\omega_m) = T_m - T_{em} - d\omega_m \tag{9}$$

In the above-given expression,  $T_m$  which is considered as a mechanical torque, as well as  $T_{em}$ , is an electromagnetic torque can be assessed using “Eq. (11)” and “Eq. (12)”, where  $p$  and  $\omega$  express correspondingly a couple of poles number and speed of the hydraulic turbine.

$$\omega_m = K_g \cdot \omega \tag{10}$$

$$T_m = \frac{T_{hydro}}{K_g} \tag{11}$$

$$T_m = pM(i_{sq}i_{rd} - i_{sd}i_{rq}) \tag{12}$$

where  $K_g$  as the gearbox ratio.

Coupling between the turbine rotors is offered by the shaft system. *4.1. Modeling of DFIG*

The shaft dynamics must be incorporated in the simulation models and it is very essential as the speed of turbines is variable also resulting Shaft oscillations and power instabilities. Alternatively, the moment of inertia of the high-speed shaft is presented in “Eq. (13)” and in the expression,  $J_i$  denotes universal inertia in  $\text{kgm}^2$ , as well as  $K_g$ , denotes the ratio of the gearbox.

$$J_i = \frac{J_{turbine}}{K_g^2} + J_{DFIG} \tag{13}$$

**4. Modeling and Control Strategy of DFIG**

one is to offer the constant voltage and frequency at stator whatever the speed deviations and rational energy feedings when the system is in a secluded area [21]. The other one is consists constant reactive power and active power during the time when the grid and generator are linked together. The stability performances of DFIG is very much good as well as its response is also faster. The oscillations in real power is less and in the reactive power is high [8].

DFIG dynamic model in (d, q) form is illustrated via “Eq. (14)” and “Eq. (15)”, where  $R_s, R_r, L_s, L_r$ , and  $M$  indicate the constraints, which are given in Appendix A.

$$\begin{bmatrix} v_{ds} \\ v_{qs} \end{bmatrix} = \begin{bmatrix} R_s & 0 \\ 0 & R_s \end{bmatrix} \begin{bmatrix} i_{ds} \\ i_{qs} \end{bmatrix} + \frac{d}{dt} \begin{bmatrix} \psi_{ds} \\ \psi_{qs} \end{bmatrix} + \begin{bmatrix} 0 & -\omega_e \\ \omega_e & 0 \end{bmatrix} \begin{bmatrix} \psi_{ds} \\ \psi_{qs} \end{bmatrix} \tag{14}$$

$$\begin{bmatrix} v_{dr} \\ v_{qr} \end{bmatrix} = \begin{bmatrix} R_r & 0 \\ 0 & R_r \end{bmatrix} \begin{bmatrix} i_{dr} \\ i_{qr} \end{bmatrix} + \frac{d}{dt} \begin{bmatrix} \psi_{dr} \\ \psi_{qr} \end{bmatrix} + \begin{bmatrix} 0 & -(\omega_e - P\omega_r) \\ (\omega_e - P\omega_r) & 0 \end{bmatrix} \begin{bmatrix} \psi_{dr} \\ \psi_{qr} \end{bmatrix} \tag{15}$$

$$T_{em} = \frac{3}{2} P \begin{bmatrix} \psi_{ds} & \psi_{qs} \end{bmatrix} \begin{bmatrix} i_{qs} \\ -i_{ds} \end{bmatrix} \tag{16}$$

The fluxes linkage equations are specified as in “Eq. (17)” and “Eq. (18)”

$$\begin{bmatrix} \psi_{ds} \\ \psi_{qs} \end{bmatrix} = \begin{bmatrix} L_s & 0 \\ 0 & L_s \end{bmatrix} \begin{bmatrix} i_{ds} \\ i_{qs} \end{bmatrix} + \begin{bmatrix} L_m & 0 \\ 0 & L_m \end{bmatrix} \begin{bmatrix} i_{dr} \\ i_{qr} \end{bmatrix} \tag{17}$$

As compared to synchronous generator, DFIG cultivates more real power as well as by inserting inconstant voltage and frequency to the rotor controls the power factor. Decoupling of the both real and reactive is also possible with the assistance of DFIG [9]. The regulating realization of the DFIG plays a vivacious role in partial load operation. DFIG facilitates to enhance the formed power in the situation of the energy production by means of a hydraulic turbine. Certainly, considering the variable speeds and the rivers in the equatorial areas, the DFIG permits compensating for these deviations in adequate amounts while guarantying a decent quality of the microgrid. The control strategy is based on two cases. The initial

$$\begin{bmatrix} \psi_{dr} \\ \psi_{qr} \end{bmatrix} = \begin{bmatrix} L_m & 0 \\ 0 & L_m \end{bmatrix} \begin{bmatrix} i_{ds} \\ i_{qs} \end{bmatrix} + \begin{bmatrix} L_r & 0 \\ 0 & L_r \end{bmatrix} \begin{bmatrix} i_{dr} \\ i_{qr} \end{bmatrix} \tag{18}$$

where  $L_s = L_m + L_{ls}$  and  $L_r = L_m + L_{lr}$  “Eq. (17)” and “Eq. (18)” can be written in terms of current equations as:

$$\begin{bmatrix} i_{qs} \\ i_{qr} \end{bmatrix} = \begin{bmatrix} \frac{1}{\sigma L_s} & -\frac{L_m}{\sigma L_s L_r} \\ -\frac{L_m}{\sigma L_s L_r} & \frac{1}{\sigma L_r} \end{bmatrix} \begin{bmatrix} \psi_{qs} \\ \psi_{qr} \end{bmatrix} \tag{19}$$

$$\begin{bmatrix} i_{ds} \\ i_{dr} \end{bmatrix} = \begin{bmatrix} \frac{1}{\sigma L_s} & -\frac{L_m}{\sigma L_s L_r} \\ -\frac{L_m}{\sigma L_s L_r} & \frac{1}{\sigma L_r} \end{bmatrix} \begin{bmatrix} \psi_{ds} \\ \psi_{dr} \end{bmatrix} \tag{20}$$

In the “Eq.(19)” and “Eq.(20)”,  $\sigma$  is the leakage coefficient  $\sigma = 1 - \frac{L_m^2}{L_r L_s}$ . The inconstant of state space in the DFIG

system is commonly fluxes or currents, in “Eq.(21)”, the inconstant of state space for the DFIG has been imitative in the arrangement of flux linkages[22]. The dynamics of the DFIG are delineated in the matrix configuration of state variables as:

$$\frac{d}{dt} \begin{bmatrix} \psi_{qs} \\ \psi_{ds} \\ \psi_{qr} \\ \psi_{dr} \end{bmatrix} = \begin{bmatrix} -c_1 & -\omega_e & c_2 & 0 \\ \omega_e & -c_1 & 0 & c_2 \\ c_3 & 0 & c_4 & (\omega_e - P\omega_r) \\ 0 & c_3 & (\omega_e - P\omega_r) & -c_4 \end{bmatrix} \begin{bmatrix} \psi_{qs} \\ \psi_{ds} \\ \psi_{qr} \\ \psi_{dr} \end{bmatrix} + \begin{bmatrix} 1 & 0 & 0 & 0 \\ 0 & 1 & 0 & 0 \\ 0 & 0 & 1 & 0 \\ 0 & 0 & 0 & 1 \end{bmatrix} \begin{bmatrix} v_{qs} \\ v_{ds} \\ v_{qr} \\ v_{dr} \end{bmatrix} \quad (21)$$

where  $c_1 = \frac{R_s}{\sigma L_s}$ ,  $c_2 = \frac{R_s L_m}{\sigma L_s L_r}$ ,  $c_3 = \frac{R_r L_m}{\sigma L_s L_r}$  and  $c_4 = \frac{R_r}{\sigma L_r}$

In “Eq. (22)”, the inconstant of state space for the DFIG has been imitative in the arrangement of rotor current and flux

**5. PI Controller Design for Rotor Side Converter of DFIG**

The control structure of a rotor of the DFIG embraces the two types of loops. The initial one is an inner loop and the other is an outer loop. The function of the inner loop is to manage the rotor components of d-axis and q-axis which is defined as the  $i_{dr}$  and  $i_{qr}$  separately and the function of other one is to manage the reactive and active power of the stator distinctly. The value of  $v_{ds}$  is equal to zero and the value of  $v_{qs}$  is equal to  $v_s$  as the spinning reference frame of the q-axis is allied to the voltage the stator. The proportional-integral controller is used for controlling the stator side flux. The flux in d-axis  $\psi_{ds}$  is equal to  $\psi_s$  in the consideration. For the de-coupled governor of reactive power and active power as designated below [21].

(Now we assume  $s=d/dt$ ).

$$\begin{cases} s\psi_{qs} + c_1\psi_{qs} = v_{qs} + c_2\psi_{qr} - \omega_e\psi_{ds} \\ \sigma\psi_{qs} = v_{qs} + c_2\psi_{qr} - \omega_e\psi_{ds} \\ \psi_{ds}^* = \frac{1}{\omega_e} (v_{qs} + c_2\psi_{qr} - \sigma\psi_{qs}) \end{cases} \quad (23)$$

$$\begin{cases} s\psi_{ds} + c_1\psi_{ds} = v_{ds} + \omega_e\psi_{qs} + c_2\psi_{dr} \\ \sigma\psi_{ds} = v_{ds} + \omega_e\psi_{qs} + c_2\psi_{dr} \\ \psi_{qs}^* = \frac{1}{\omega_e} (\sigma\psi_{ds} - c_2\psi_{dr} - v_{ds}) \end{cases} \quad (24)$$

here  $\sigma\psi_{qs} = c_1\psi_{qs} + s\psi_{qs} = \frac{K_{I\psi_s}}{s} (\psi_{qs}^* - \psi_{qs}) + K_{p\psi_s}$  and  $\sigma\psi_{ds} = c_1\psi_{ds} + s\psi_{ds} = \frac{K_{I\psi_s}}{s} (\psi_{ds}^* - \psi_{ds}) + K_{p\psi_s}$  are the outputs from the Proportional Integral controllers.

linkages of the stator. The dynamics of the DFIG are delineated in the matrix configuration of state variables as:

$$\frac{d}{dt} \begin{bmatrix} \psi_{qs} \\ \psi_{ds} \\ i_{qr} \\ i_{dr} \end{bmatrix} = \begin{bmatrix} -K_1 & -\omega_e & 0 & K_2 \\ \omega_e & -K_1 & K_2 & 0 \\ 0 & -K_3 & K_4 & -\omega_{sl} \\ -K_3 & 0 & \omega_{sl} & -K_4 \end{bmatrix} \begin{bmatrix} \psi_{qs} \\ \psi_{ds} \\ i_{qr} \\ i_{dr} \end{bmatrix} + \begin{bmatrix} 1 & 0 & 0 & 0 \\ 0 & 1 & 0 & 0 \\ 0 & 0 & K_5 & 0 \\ 0 & 0 & 0 & K_5 \end{bmatrix} \begin{bmatrix} v_{qs} \\ v_{ds} \\ v_{qr} \\ v_{dr} \end{bmatrix} \quad (22)$$

where  $K_1 = \frac{R_s}{L_s}$ ,  $K_2 = \frac{R_s L_m}{L_s}$ ,  $K_3 = \frac{\omega_{sl} L_m}{\sigma L_r L_s}$ ,  $K_4 = \frac{R_r}{\sigma L_r}$  and  $K_5 = \frac{1}{\sigma L_r}$

The PI controller is determined by equating with the Butterworth polynomial which is described below as:

$$K_{p\psi_s} = 1.414\omega_o - \frac{R}{\sigma L_s} \quad (25)$$

$$K_{l\psi_s} = \omega_o^2 \quad (26)$$

where  $P_r$  is a nominal power of the hydraulic turbine and  $\omega_r$  is the nominal speed of the hydraulic turbine.

“Equation (23)” can be re-written as

$$\frac{2J}{P_r} s\omega_{rs} = (T_m - T_{em}) = \sigma_{wr} = K_{wr} (\omega_{rs}^* - \omega_{rs}) \quad (27)$$

where  $K_{wr}$  is the gain of PI controller for rotor speed controller, specified as

$$K_{wr} = (K_{pwr} + \frac{K_{lwr}}{s}) \quad (28)$$

Then “Eq. (27)” will be

$$\begin{cases} \frac{2J}{P_r} s\omega_{rs} = (K_{pwr} + \frac{K_{lwr}}{s})\omega_{rs}^* - (K_{pwr} + \frac{K_{lwr}}{s})\omega_{rs} \\ \frac{\omega_{rs}}{\omega_{rs}^*} = \frac{\frac{P_r}{2J} (s K_{pwr} + K_{lwr})}{s^2 + s \frac{P_r K_{pwr}}{2J} + \frac{P_r K_{lwr}}{2J}} \end{cases} \quad (29)$$

The closed loop electrical subsystem with PI controller for rotor speed is as shown in “figure (4)” [23].

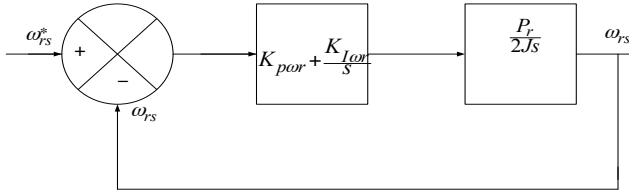


Fig. 4. PI controller for the speed of the rotor

Now equating the denominator of “Eq. (29)” with standard second order equation  $s^2 + 2\zeta\omega_n s + \omega_n^2$

$$\omega_n^2 = \frac{P_r K_{Iwor}}{2J} \quad \text{and} \quad 2\zeta\omega_n = \frac{P_r K_{Pwor}}{2J}$$

We assume the natural frequency is 60 rad/sec and system is critically damped so  $\zeta = 1$

$$(60)^2 = \frac{2 \times 10^6 \times K_{Iwor}}{2 \times 3.82}$$

$$K_{Iwor} = 0.0137 \quad \text{and}$$

$$2 \times 1 \times 60 = \frac{2 \times 10^6 \times K_{Pwor}}{2 \times 3.82}$$

$$K_{Pwor} = 0.00045$$

Substituting  $\psi_{qs}=0$  in “Eq. (16)” and “Eq. (17)” results in “Eq. (30)”

$$\begin{cases} T_{em} = 1.5\psi_{ds}i_{qs} \\ i_{qs} = -\frac{L_m}{L_s}i_{qr} \end{cases} \quad (30)$$

A further substitution of “Eq. (29)” into “Eq. (27)” and in combination with “Eq. (26)” results in:

$$T_{em} = 1.5\psi_{ds} \left(-\frac{L_m}{L_s}\right)i_{qr} \quad (31)$$

$$i_{qr} = \frac{2}{3}(\sigma_{wr} - T_m) \frac{L_s}{\psi_{ds}L_m} \quad (32)$$

Now, the real power by stator is specified as:

$$P_s = 1.5(v_{qs}i_{qs} + v_{ds}i_{ds}) = -1.5 \frac{L_m}{L_s} v_{qs}i_{qr} \quad (33)$$

Now, the reactive power provided by stator is specified as:

$$Q_s = 1.5(v_{qs}i_{ds} - v_{ds}i_{qs}) = 1.5v_{qs}i_{ds} \quad (34)$$

Substituting  $v_{qs}$  in “Eq. (32)” gives:

$$Q_s = 1.5(R_s i_{qs} + \omega_e \psi_{ds} + s\psi_{qs})i_{ds} \quad (35)$$

Stator flux is assumed to be constant, neglecting the stator resistance and substituting  $i_{ds}$  from “Eq. (20)” gives

$$Q_s = 1.5\left(\psi_{ds}^2 - \frac{L_m}{L_r}\psi_{ds}\psi_{dr}\right) \frac{\omega_e}{\sigma L_s} \quad (36)$$

Differentiating “Eq. (34)” w. r. t. time provides

$$sQ_s = -1.5 \frac{\omega_e}{\sigma L_s} \frac{L_m}{L_r} \psi_{ds} s\psi_{dr} \quad (37)$$

From “Eq. (35)” and “Eq. (15)” and solving  $\psi_{qr}$  in terms of  $i_{qr}$  provides the “Eq. (38)”

$$\begin{cases} sQ_s = -1.5 \frac{\omega_e}{\sigma L_s} \frac{L_m}{L_r} \psi_{ds} (v_{dr} + (\omega_e - \omega_r)\psi_{qr} - R_r i_{dr}) \\ sQ_s = -1.5 \frac{\omega_e}{\sigma L_s} \frac{L_m}{L_r} \psi_{ds} (v_{dr} + (\omega_e - \omega_r)\sigma L_r i_{qr} - R_r i_{dr}) \\ \mu s Q_s = (Q_s^* - Q_s) K_{Qs} = \sigma Q_s \end{cases} \quad (38)$$

where  $\mu$  is defined as  $\mu = \frac{2L_r L_s \sigma}{3L_m \omega_e}$  and  $K_{Qs}$  is the gain of PI controller for reactive power of the stator side, provides as:

PI controller for reactive power of the stator side, provides as:

$$K_{Qs} = (K_{PQs} + \frac{K_{IQs}}{s})$$

Therefore “Eq. (38)” can be modified as given below:

$$\mu s Q_s = \left(\frac{K_{IQs}}{s} + K_{PQs}\right) Q_s^* - \left(\frac{K_{IQs}}{s} + K_{PQs}\right) Q_s \quad (39)$$

$$\frac{Q_s}{Q_s^*} = \frac{\frac{1}{\mu} (sK_{PQs} + K_{IQs})}{s^2 + s \frac{K_{PQs} + K_{IQs}}{\mu}} \quad (40)$$

The closed loop electrical subsystem with PI controller for stator side reactive power as shown in “figure(5)”[23].

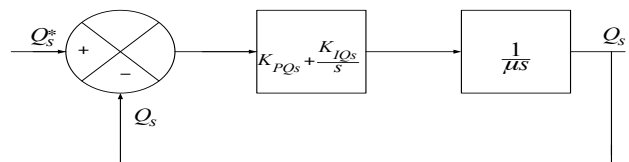


Fig. 5. PI controller for reactive power of the stator

Now equate the denominator of “Eq. (40)” with standard second order equation  $s^2 + 2\zeta\omega_n s + \omega_n^2$

$$\omega_n^2 = \frac{K_{IQs}}{\mu}$$

$$(60)^2 = \frac{K_{IQs}}{3.74 \times 10^{-7}}$$

$$K_{IQs} = 0.00134 \text{ and}$$

$$2\xi\omega_n = \frac{K_{PQs}}{\mu}$$

$$2 \times 1 \times 60 = \frac{K_{PQs}}{3.74 \times 10^{-7}}$$

$$K_{PQs} = 0.000044$$

From “Eq. (37)” and “Eq. (38)” gives

$$i_{dr}^* = \frac{1}{R_r} (v_{dr} + \frac{\sigma Q_s}{\psi_{ds}} + \sigma L_r i_{qr} (\omega_e - \omega_r)) \quad (41)$$

From “Eq. (31)” and “Eq. (41)”, active stator power and reactive stator power are proportionate to the rotor current in q-axis i.e.  $i_{qr}$ . The mutual coupling term  $\omega_{sl} \sigma i_{qr} L_r$  in “Eq. (41)” is very small so its consequence is insignificant. The current of the rotor can be regulated by the assistance of rotor voltages. The relation between rotor current and rotor voltage is attained by replacing values of  $\psi_{dr}$  as well as  $\psi_{qr}$  from “Eq. (18)” in “Eq. (15)” and additional interpretation yields:

$$v_{qr} = R_r i_{qr} + \omega_{sl} \left( \frac{L_m}{L_s} \psi_{ds} + \sigma L_r i_{dr} \right) + \sigma L_r s i_{qr} \quad (42)$$

$$v_{dr} = R_r i_{dr} - \omega_{sl} \sigma L_r i_{qr} + \sigma L_r s i_{dr} \quad (43)$$

where  $\omega_{sl}$  is defined as the slip speed  $\omega_{sl} = (\omega_e - \omega_r)$  and

$$\sigma = 1 - \frac{L_m^2}{L_s L_r}$$

In “Eq. (42)” and “Eq. (43)”, there is the term counting  $i_{dr}$  in the d-axis expression and there is the term counting  $i_{qr}$  in the q-axis expression. So the two expressions are attached and the outmoded linear controllers is not apposite. However, with the assistance of the exact linearization method, the equations can be linearized by placing the terms other than the currents control to one side.

$$R_r i_{qr} + \sigma L_r s i_{qr} = v_{qr} - \omega_{sl} \left( \frac{L_m}{L_s} \psi_{ds} + \sigma L_r i_{dr} \right) \quad (44)$$

$$R_r i_{dr} + \sigma L_r s i_{dr} = v_{dr} + \omega_{sl} (\sigma L_r i_{qr}) \quad (45)$$

Then the currents can be structured by linear controllers, where

$$\sigma_{qr} = R_r i_{qr} + \sigma L_r s i_{qr} \quad (46)$$

$$\sigma_{dr} = R_r i_{dr} + \sigma L_r s i_{dr} \quad (47)$$

The view behind this is to use the linear controllers that embrace integration for computing the derivative expressions. The nonlinear equations can be altering to a linear equation by moving wholly the nonlinear terms to the other side of the equations. Then the voltages of d-axis and q-axis are designed as presented below.

$$v_{qr}^* = \sigma_{qr} + \omega_{sl} \left( \frac{L_m}{L_s} \psi_{ds} + \sigma L_r i_{dr} \right) \quad (48)$$

$$v_{dr}^* = \sigma_{dr} - \omega_{sl} (\sigma L_r i_{qr}) \quad (49)$$

DFIG is secured by an inner current control loop due to its momentous advantage. Inner current control loop can undoubtedly shield the system from excess current because current controllers can be simply implanted in the control scheme. Since PI controllers are extensively used and it is very much operative, they are furthermore used in the subsequent exploration. So for finding rotor current in q-axis  $i_{qr}$  by means of current regulator loop from “Eq. (44)”.

$$v_{qr}^* = R_r i_{qr} + \sigma L_r s i_{qr} = (R_r + s \sigma L_r) i_{qr} \quad (50)$$

$$v_{qr}^* = \left( K_{qp} + \frac{K_{qi}}{s} \right) (i_{qr}^* - i_{qr}) \quad (51)$$

$$(R_r + s \sigma L_r) i_{qr} = \left( K_{qp} + \frac{K_{qi}}{s} \right) i_{qr}^* - \left( K_{qp} + \frac{K_{qi}}{s} \right) i_{qr} \quad (52)$$

Likewise, for finding  $i_{dr}$  by means of current regulator loop from “Eq. (45)”:

$$v_{dr}^* = R_r i_{dr} + \sigma L_r s i_{dr} = (R_r + s \sigma L_r) i_{dr} \quad (53)$$

$$v_{dr}^* = \left( K_{qp} + \frac{K_{qi}}{s} \right) (i_{dr}^* - i_{dr}) \quad (54)$$

$$(R_r + s \sigma L_r) i_{dr} = \left( K_{qp} + \frac{K_{qi}}{s} \right) i_{dr}^* - \left( K_{qp} + \frac{K_{qi}}{s} \right) i_{dr} \quad (55)$$

Now the transfer function from “Eq. (55)” amid the reference and authentic currents are rehabilitated as given below:

$$\begin{aligned} \frac{i_{qr}}{i_{qr}^*} &= \frac{K_{qi} + s K_{qp}}{s^2 \sigma L_r + s(K_{qp} + R_r) + K_{qi}} \\ &= \frac{\frac{1}{\sigma L_r} (s K_{qp} + K_{qi})}{s^2 + s \frac{1}{\sigma L_r} (K_{qp} + R_r) + \frac{1}{\sigma L_r} K_{qi}} \end{aligned} \quad (56)$$

The closed loop electrical subsystem with PI controller for rotor

q-axis and d-axis currents as shown in “figure (6)” and “figure (7)”[23].

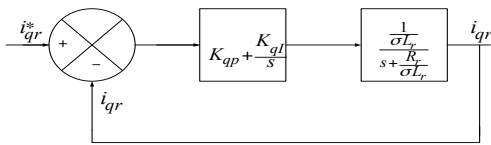


**Fig. 6.** PI controllers for q-axis current of the rotor

Now equating the denominator of “Eq.(56)” with standard second order equation  $s^2 + 2\zeta\omega_n s + \omega_n^2$

$$\frac{i_{dr}}{i_{dr}^*} = \frac{sK_{dp} + K_{di}}{s^2\sigma L_r + s(R_r + K_{dp}) + K_{di}}$$

$$= \frac{\frac{1}{\sigma L_r}(sK_{dp} + K_{di})}{s^2 + s\frac{1}{\sigma L_r}(R_r + K_{dp}) + \frac{1}{\sigma L_r}K_{di}} \quad (57)$$

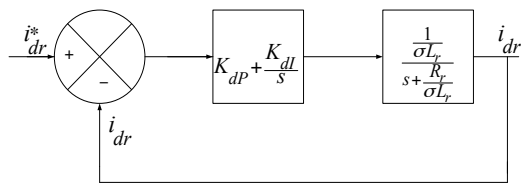


**Fig.7.** PI controllers for d-axis current of the rotor

Now equate the denominator of “Eq. (57)” with standard second order equation  $s^2 + 2\zeta\omega_n s + \omega_n^2$

$$\omega_n^2 = \frac{K_{dl}}{\sigma L_r} \text{ so put all the values}$$

$$(60)^2 = \frac{K_{dl}}{0.066 \times 0.002587}$$

$$K_{dl} = 0.6146 \text{ and}$$

$$2 \times 1 \times 60 = \frac{0.0029 + K_{dp}}{0.066 \times 0.002587}$$

$$K_{dp} = 0.0175$$

To retain the entire system in the stable area as well as to find the system constraints there are a few methods which were used. Butterworth polynomial was used to adjust the Eigenvalues of a closed loop. In this method, the system stability is resolved by assigning the roots of closed loop auxiliary equation in the left half s-plane on a circle with

$$\omega_n^2 = \frac{K_{ql}}{\sigma L_r} \text{ so laid all the values}$$

$$(60)^2 = \frac{K_{ql}}{0.066 \times 0.002587}$$

$$K_{ql} = 0.6146 \text{ and}$$

$$2 \times 1 \times 60 = \frac{0.0029 + K_{qp}}{0.066 \times 0.002587}$$

$$K_{qp} = 0.0175$$

radius  $\omega_0$  and pictorial representation shown in “figure (9)” [24].

$$s^2 + \sqrt{2}\omega_0 s + \omega_0^2 = 0 \quad (58)$$

In “Eq.(58)”  $\omega_0$  is engaged as the bandwidth of the current controller and it leans on the design value. A Pictorial representation of Rotor side controller (RSC) control scheme is presented in “Figure (8)” [25].

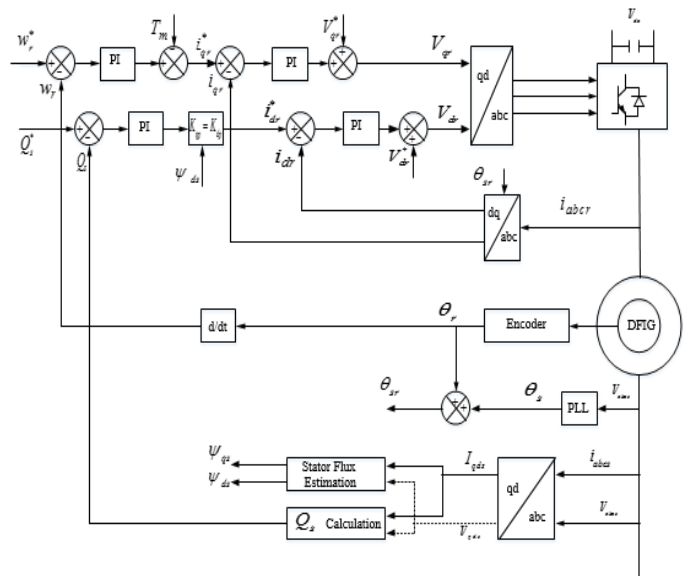


**Fig. 8.** Pictorial representation of rotor side controller (RSC) control scheme

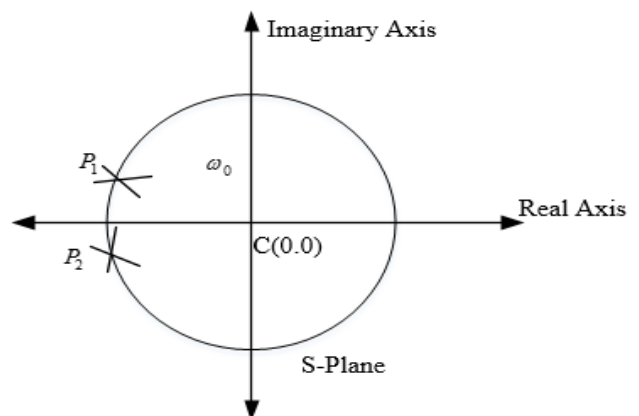


**Fig. 9.** Representation of poles location of a second order Butterworth polynomial in s-plane.

$$v_{dr}^{comp} = -\omega_{sl} \sigma L_r i_{qr} \quad \text{And}$$

$$v_{dr}^{comp} = \omega_{sl} \left( \frac{L_m}{L_s} \psi_{ds} + \sigma L_r i_{qr} \right)$$

**6. PI Controller design for the Grid Side Converter of DFIG**

The reactive power which is an alteration between the converter and grid, as well as the voltage across the capacitor, is controlled by the control mechanism of grid side converter (GSC). Producing unity power factor in the joining node of the grid and to control the DC link voltage of the converter to an invariable value are the focal moto in the grid side [26]. To conquer the unity power factor at the grid side, we have to regulate the d-axis current so for this purpose, PI controller is very much crucial here. Grid side converter embraced two control loops. So q-axis current is controlled by interior loop by the means of PI controller as well as DC link voltage is regulated by exterior loop by the means of second PI controller. Grid side converter (GSC) control mechanism is subsequent as:

1. In the grid side converter (GSC) active power is controlled by regulating the dc link voltage ( $v_{dc}$ ).
2. The voltage of DC bus plays a vivacious role in the monitoring of the active power of GSC. The active power of the rotor is wholly delivered to the grid without any wasted in DC bus capacitor by guardianship the DC bus voltage is constant [27, 28].
3. Terminal voltage, power factor and reactive power of the stator are deliberated as control variables and grid side converter also embraces the reactive power control [29].
4. The output of the controller is either a d-q component of the reference voltage or d-q component of the reference current to the pulse width modulation (PWM) of grid side converter (GSC) [30].

The dc-link voltage can be specified as:

$$C s v_{dc} = \frac{3}{4} (M_{qr} i_{qr} + M_{dr} i_{dr}) + \frac{3}{4} (M_{df} i_{df} + M_{qf} i_{qf}) \quad (59)$$

$$C s v_{dc} = \frac{3}{4} (M_{qr} i_{qr} + M_{dr} i_{dr}) + \frac{3}{4} (M_{df} i_{df} + M_{qf} i_{qf}) \quad (60)$$

$$= \sigma_{dc}$$

“Equation (60)” can be revised as:

$$C_{dc} s v_{dc} = \sigma_{dc} = K_{dc} (v_{dc}^* - v_{dc}) \quad (61)$$

In the above expression,  $K_{dc}$  is considered as the gain of the PI controller for DC bus voltage control specified as:

$$K_{dc} = \left( K_{pdc} + \frac{K_{Idc}}{s} \right)$$

Then “Eq. (61)” will be presented as:

$$C_{dc} s v_{dc} = \left( K_{pdc} + \frac{K_{Idc}}{s} \right) v_{dc}^* - \left( K_{pdc} + \frac{K_{Idc}}{s} \right) v_{dc} \quad (62)$$

$$\frac{v_{dc}}{v_{dc}^*} = \frac{1}{s^2 + s \frac{K_{pdc}}{C_{dc}} + \frac{K_{Idc}}{C_{dc}}} \quad (63)$$

The closed loop electrical subsystem with PI controller for dc voltage of grid side as shown in “figure (10)” [23].

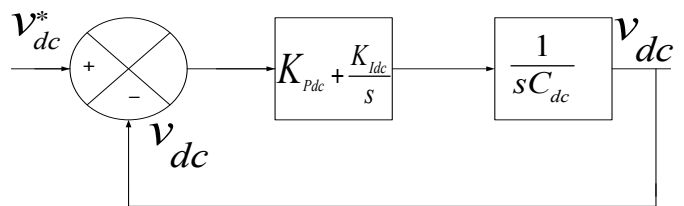


**Fig.10.** PI controllers for dc voltage for grid side converter

Equating the denominator of “Eq. (63)” with standard second order polynomial, i.e.  $s^2 + 2\xi\omega_n s + \omega_n^2$ , PI controller gains are acquired as:

$$\omega_n^2 = \frac{K_{Idc}}{C_{dc}} \quad \text{so put } C_{dc} = 0.059 \text{ Farad}$$

$$(60)^2 = \frac{K_{Idc}}{0.059}$$

$$K_{Idc} = 212.4 \quad \text{and}$$

$$2 \times \xi \times \omega_n = \frac{K_{pdc}}{C_{dc}}$$

$$2 \times 1 \times 60 \times 0.059 = K_{pdc}$$

$$K_{pdc} = 7.08$$

From “Eq. (60)”,

$$i_{qf}^* = \frac{4}{3} \frac{1}{M_{qf}} \left( \sigma_{dc} - \frac{3}{4} (M_{qr} i_{qr} + M_{dr} i_{dr}) \right) - \frac{M_{df}}{M_{qf}} i_{df} \quad (64)$$

By means of KVL across the RL, the filter provides

$$v_{qf} = R_f i_{qf} + L_f s i_{qf} + \omega_e L_f i_{df} + \frac{v_{qs}}{K_T} \quad (65)$$

$$= M_{qf} \frac{v_{dc}}{2}$$

$$v_{df} = R_f i_{df} + L_f s i_{df} - \omega_e L_f i_{qf} \quad (66)$$

$$= M_{df} \frac{v_{dc}}{2}$$

Considering the q-axis of the spinning reference frame is allied to the voltage of stator such that the value of  $v_{qs}$  is equal to  $v_s$  and the value of  $v_{ds}$  is equal to zero. So, the grid receives the reactive power from grid side converter and this reactive power is guarded by means of a current of d-axis.

$$Q_f = \frac{1.5}{K_T} i_{df} v_s \quad (67)$$

In “Eq.(67)”  $K_T$  is deliberated as transformer turns ratio associated amid GSC and stator.

$$sQ_f = 1.5s i_{df} \frac{v_s}{K_T} \quad (68)$$

Replacing “Eq. (66)” in “Eq. (68)” gives

$$sQ_f = 1.5 \frac{v_s}{K_T L_f} (v_{df} - R_f i_{df} + \omega_e L_f i_{qf}) \quad (69)$$

$$\lambda s Q_f = (v_{df} - R_f v_{df} + \omega_e L_f i_{qf}) = \sigma_{qf} \quad (70)$$

where  $\lambda$  is well-defined as :

$$\lambda = \frac{2L_f K_T}{3v_s}$$

$$\sigma_{qf} = \lambda s Q_f = (Q_f^* - Q_f) K_{Qf} \quad (71)$$

where  $K_{Qf}$  is the gain of PI controller for reactive power delivered by grid side converter specified as:

$$K_{Qf} = K_{PQf} + \frac{K_{IQf}}{s} \quad (72)$$

Again “Eq. (71)” will be modified as:

$$\lambda s Q_f = (K_{PQf} + \frac{K_{IQf}}{s}) Q_f^* - (K_{PQf} + \frac{K_{IQf}}{s}) Q_f \quad (73)$$

$$\frac{Q_f}{Q_f^*} = \frac{\frac{1}{\lambda} (sK_{PQf} + K_{IQf})}{s^2 + s \frac{K_{PQf}}{\lambda} + \frac{K_{IQf}}{\lambda}} \quad (74)$$

The closed loop electrical subsystem with PI controller for reactive power of grid side as shown in “figure (11)” [23].

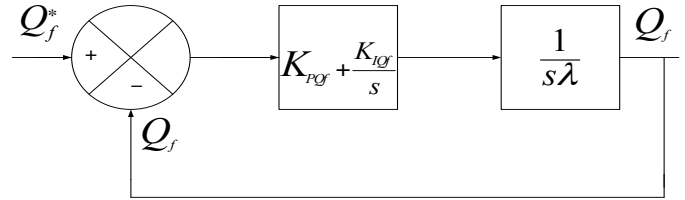


Fig.11. PI controllers for reactive power of grid side converter

Equating denominator of “Eq.(74)” with standard second order polynomial,  $s^2 + 2\xi\omega_n s + \omega_n^2$ , PI controller gains are acquired as:

$$\omega_n^2 = \frac{K_{IQf}}{\lambda} \text{ so put all the values, } \lambda = 6.37 \times 10^{-7}$$

$$(60)^2 = \frac{K_{IQf}}{6.37 \times 10^{-7}}$$

$$K_{IQf} = 0.0023 \text{ and}$$

$$2 \times \xi \times \omega_n = \frac{K_{PQf}}{\lambda}$$

$$2 \times 1 \times 60 = \frac{K_{PQf}}{6.37 \times 10^{-7}}$$

$$K_{PQf} = 0.000076$$

From “Eq. (70)”

$$i_{df}^* = \frac{1}{R_f} (v_{df} + \omega_e L_f i_{qf} - \sigma_{qf}) \quad (75)$$

Equation (65) and “Eq. (66)” add the innermost current control loop for the grid side converter regulation.

On the assumption that:

$$R_f i_{qf} + L_f s i_{qf} = K_{qf} (i_{qf}^* - i_{qf}) = \sigma_{qf} \quad (76)$$

$$R_f i_{df} + L_f s i_{df} = K_{df} (i_{df}^* - i_{df}) = \sigma_{df} \quad (77)$$

Then “Eq. (65)” and “Eq. (66)” can be inscribed below

$$M_{qf} = \frac{2}{v_{dc}} (\sigma_{qf} + \frac{v_{qs}}{K_T} + \omega_e L_f i_{df}) \quad (78)$$

$$M_{df} = \frac{2}{v_{dc}} (\sigma_{df} - \omega_e L_f i_{qf}) \quad (79)$$

“Equation (78)” and “Eq. (79)” contribute modulation indicators and these indicators are providing the output of the given converter.  $K_{df}$  and  $K_{qf}$  are gain of the PI current controllers for d-axis and q-axis currents, correspondingly so

$$K_{df} = K_{qf} = K_{p1} + \frac{K_{I1}}{s} \quad (80)$$

Then “Eq. (76)” can be re-written as

$$\frac{i_{qf}}{i_{qf}^*} = \frac{\frac{1}{L_f} (sK_{p1} + K_{I1})}{s^2 + s \frac{1}{L_f} (R_f + K_{p1}) + \frac{1}{L_f} K_{I1}} \quad (81)$$

The closed loop electrical subsystem with PI controller for q-axis current of grid side as shown in “figure (12)” [23].

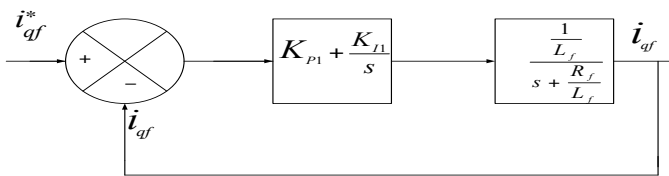


**Fig. 12.** PI controller for q-axis current of grid side

Equating the denominator of “Eq. (81)” with the basic second order polynomial  $s^2 + 2\zeta\omega_n s + \omega_n^2$  gives:

$$\omega_n^2 = \frac{K_{I1}}{L_f} \text{ so } (60)^2 = \frac{K_{I1}}{2 \times 10^{-3}}$$

$$K_{I1} = 7.2 \text{ and}$$

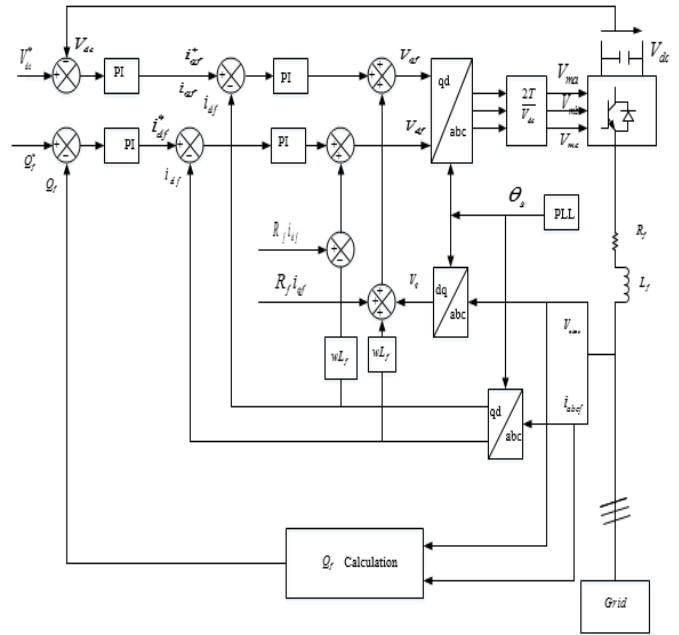
$$2\zeta\omega_n = \frac{R_f + K_{p1}}{L_f}$$

$$R_f = 6.3 \times 10^{-3} \Omega$$

$$2 \times 1 \times 60 = \frac{6.3 \times 10^{-3} + K_{p1}}{2 \times 10^{-3}}$$

$$K_{p1} = 0.2337$$

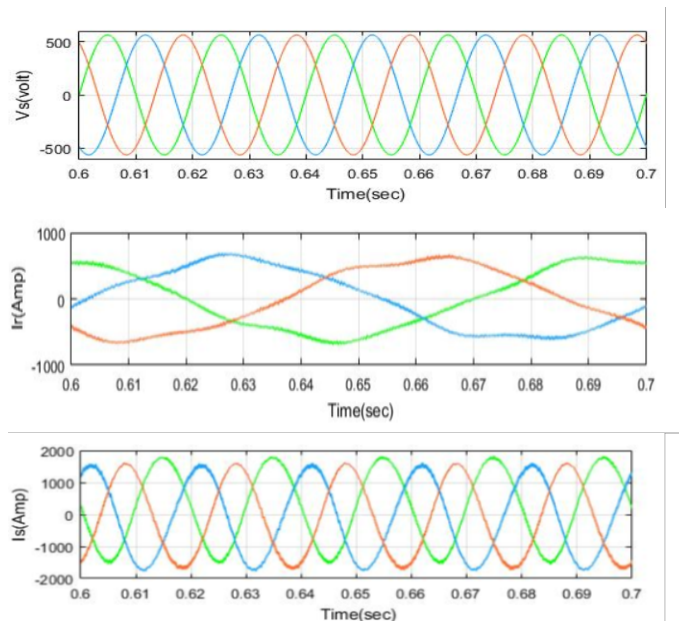
The GSC control arrangement is displayed below in “Figure. 13” [25].

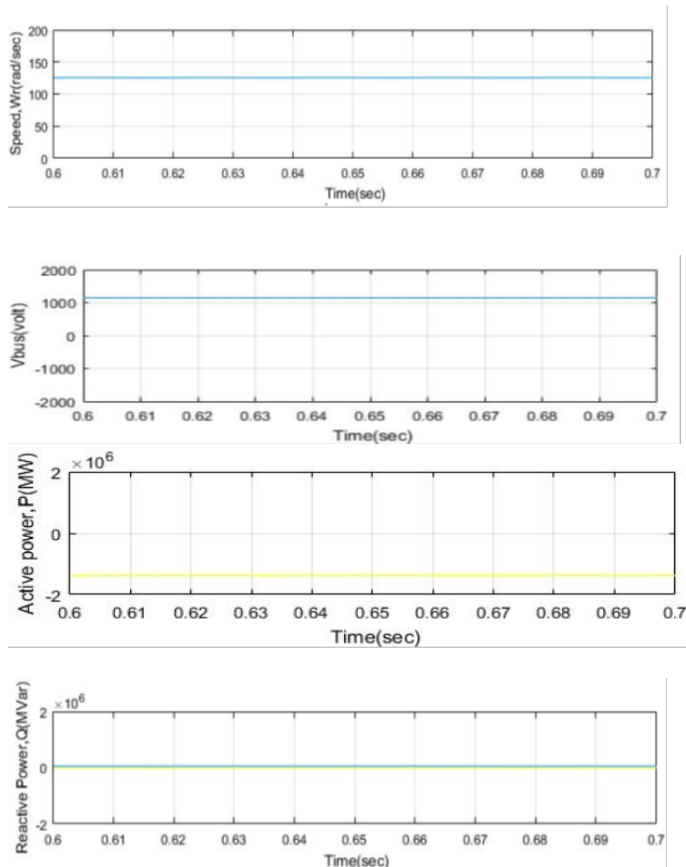


**Fig.13.** Pictorial representation of Grid side controller control scheme

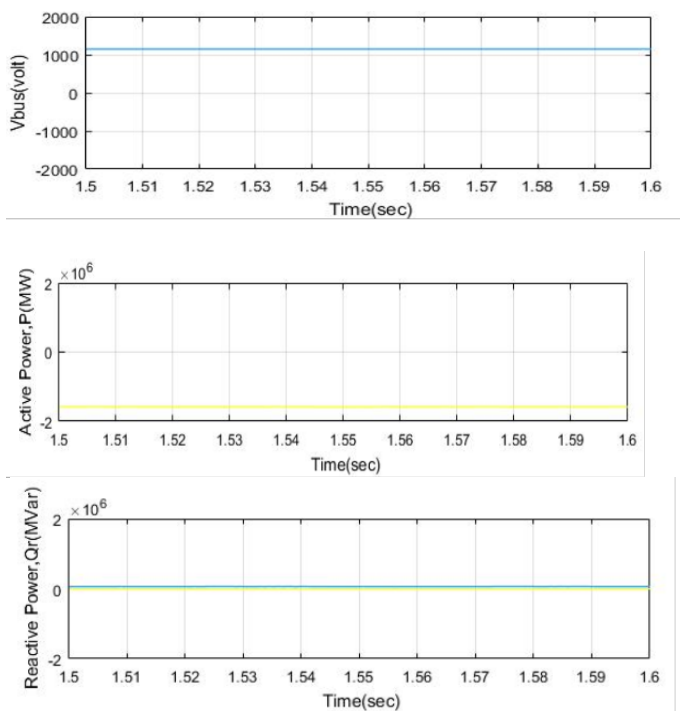
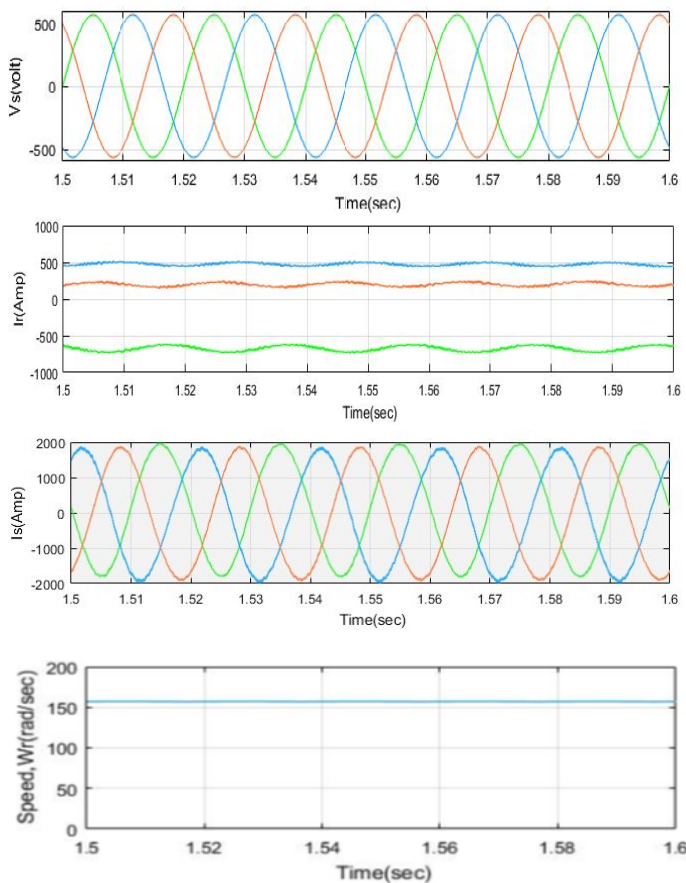
### 7. Results and discussion

A PI control scheme is implemented on the simulation model and the analysis of simulated result is completed in the terms of real and reactive power and converter rating. “Figures 14-16” presented the waveforms for 2 MW SHPP using a back to back converter associated with DFIG at different modes of operation. Here DFIG is used to increase the power saving, reduce the loss of machine and for improving the overall efficiency. These ultimate features of DFIG establish the differences from those generators which are currently used in India. For corroboration of operation conditions, rotor current, stator current, supply voltage, and DC bus voltage are shown by the waveform. All the results are tabulated in Table 1.

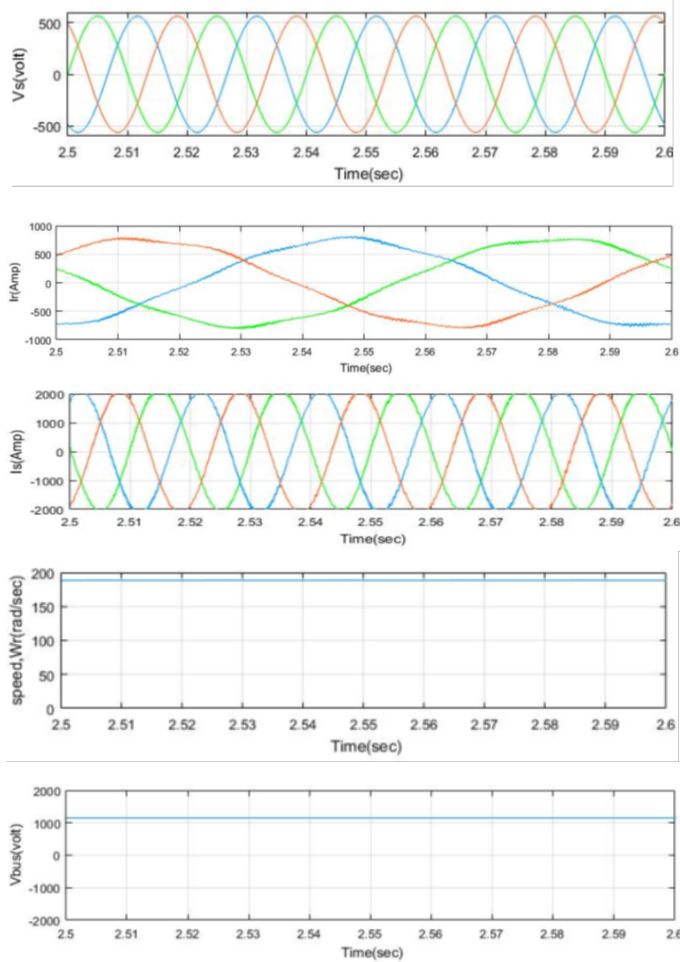




**Fig.14.** Performance of 2 MW SHPP associated with DFIG at sub-synchronous speed (Speed of the rotor=125.6rad/sec)



**Fig.15.** Performance of 2 MW SHPP associated with DFIG at synchronous speed (Speed of the rotor=157rad/sec)



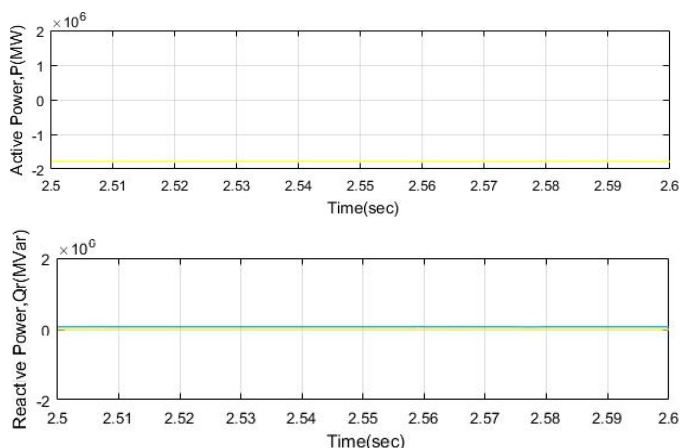


**Fig.16.** Performance of 2 MW SHPP associated with DFIG at super-synchronous speed (Speed of the rotor=188.4rad/sec)

**Table1.** Assessment of the performance of a 2 MW SHPP associated with DFIG at different speed modes

$\omega_r$ (rad/se c)	$I_{sf}$ (A z)	$I_{rf}$ (A z)	$P_{out}$ (M W)	$Q_{out}$ (MVar r)	$v_s$ (Vol t)	$v_{bus}$ (Volt )	$Q_{grid}$ (MV ar)
125.6	50	10	-1.3	00	690	1150	00
157	50	00	-1.6	00	690	1150	00
188.4	50	-10	-1.7	00	690	1150	00

## 8. Conclusion

Due to copious advantages as compared to another form of energy, grid-integrated small hydropower plant is being implemented in the existing scenario. In this paper, a complete simulation model of a back to back converter fed DFIG for 2 MW SHPP is developed with PI controller schemes which controls the real and reactive power distinctly. Grid side converter and rotor side converter schemes are implemented here. For switching the state from sub- synchronous to super-synchronous mode, PI control method is used. MATLAB/SIMULINK is used for simulating the entire system. The copious simulated results are perceived and examined under different modes of operation and It has been found that all the simulated outcomes fulfilling all the prerequisite of small hydro power plant system. We used PI controller scheme in the rotor side as well as grid side also for superior performance. For real time situation, we can use same given model in real time digital simulator (RT-LAB) and then the result acquired from real time digital simulator, as well as the result acquired from PI controller is very much similar.

## Appendix

### A. Constraints of 2MW DFIG in Small Hydropower Plant

Constraint (Unit)	Value
Rated power (MW)	2
Stator voltage (V)/Frequency (Hz)	690/50
Stator/Rotor turns ratio	0.33
Pole pairs (P)	2
Stator resistance (ohm)	0.0026
Rotor resistance (ohm)	0.0029

Angular moment of Inertia (s)	3.82
Stator Inductance (H)	0.00258
Rotor Inductance (H)	0.00258
Mutual Inductance (H)	0.0025
Turbine rotor speed (rad/sec)	157

## Acknowledgments

This research was promoted by National Institute of Technology, Jamshedpur, India. The first and second author are obliged to associate professor Dr. Madhu Singh (NIT, Jamshedpur) for endless guidance to complete this research work.

## References

- [1] Bhide A, Monray C R, "Energy Poverty: a Special Focus on Energy Poverty in India and Renewable Energy Technologies", *Renewable Sustainable Energy Rev* 2011; 15(2): 1057-66, 2011.
- [2] Khan R, "Towards Realizing Social Sustainability in the Small Hydropower Sector in India: Opportunities for Social Innovations", *International Journal Innovative Sustainable Development* 2015:9(1): 48-62, 2015.
- [3] Mishra M K, Khare N, Agrawal A B, "Small Hydro Power in India: : Current Status and Future Perspectives", *Renewable and Sustainable Energy Reviews* 51(2015), 101-115, 2015.
- [4] Khan R, "Small Hydro Power In India: Is it a Sustainable Business?", *Appl Energy*, 152:207-16, 2015.
- [5] Government of India, "The National Electricity Plan", Ministry of New and Renewable Energy, Jan 2017.
- [6] Nautiyan H, Singal S K, Varun Sharma, "Small Hydropower for sustainable energy development in India", *Renew Sustainable Energy Rev* 2011; 15(4):2021-7, 2011.
- [7] White Paper, IEC Market Strategy Board, "Grid Integration of Large-Capacity Renewable Energy Sources and Use of Large-Capacity Electrical Energy Storage", *Report, October* 2012.
- [8] Boldea I, "Control of Electric Generators: A Review", *Industrial Electronics Society, IECON '03', The 29th Annual Conference of the IEEE*, Vol. 1, pp. 972-980, 2-3 Nov 2003.
- [9] Bendi J, Chombt M, Schreier L, "Adjustable- Speed Operation of Doubly Fed Induction Machine in Pumped Storage Power Plants," *Electrical Machines and Drives, Ninth International Conference on (Conf. Publ. No. 468)*, pp.223-227,1999.
- [10] Olimpo A L, Nick J, Janaka E, Cartwright Phill, Hughes Michael, "Wind Energy Generation: Modelling and Control", *John Willey & Sons; 24th Aug.* 2011.

- [11] Gharedaghi F, Jamali H, Deisi M, Khalili A. Modelling and Simulation of DFIG with Fault Ride Through Protection. *Australian Journal of Basic and Applied Science* 2011; vol. 5(no.6): 858-62.
- [12] Premalatha M, Abbasi T, Abbasi T, Abbasi S, "A Critical View on the Eco-Friendliness of Small Hydroelectric Installations", *SCI Total Environ*, 481 :638-43, 2014.
- [13] Erlewie A, "Disappearing Rivers-the Limits of Environmental Assessment for Hydropower in India", *Environ Impact Assess Rev*, 43, 135-43, 2013.
- [14] S.M. Barakati, M.Kazerani and J.D.Aplevich, "Maximum power tracking control for a wind turbine system including a matrix converter," *IEEE Transactions on Energy Conversion*, vol. 24, no. 3, pp.705- 713, sep.2009.
- [15] Schmidt E, Ertl J, Preiss A, Zensch R, Schurhuber R, Hell J, "Studies about the Low Voltage Ride Through capabilities of Variable- Speed Motor Generators of Pumped Storage Hydro Power Plants", *Universities Power Engineering Conference (AUPEC), 21st Australasian*, pp. 1.6, 25-28th Sept. 2011.
- [16] Kumar D, Katoch SS, "Harnessing 'Water Tower' into 'Power Tower': A Small Hydropower Development Study from an India Prefecture in Western Himalayas", *Renew Sustain Energy Rev*, 39:87- 101, 2014.
- [17] S. Bojic, D. Bozic, M. Pavlica, "Refurbishment of Small Hydro Power Plant", 2012 *International Conference on Renewable Energy Research and Applications (ICRERA)*, Nagasaki, Japan, 2012.
- [18] Nouni M R, Mullick S C, Kandapal T C, "Providing Electricity Access to Remote Areas in India: Niche Areas for Decentralized Electricity Supply", *Renew Energy* 2009; 34(2):430-4, 2009.
- [19] Bhattacharya S, Jana C, "Renewable Energy in India: Historical Developments and Prospects", *Energy* 2009; 34(8):981-91, 2009.
- [20] A. Ansel, M. Biet, B. Robyns, Micro hydropower station based on a doubly fed induction generator excited by a PM synchronous machine, in *ICEM 2004*, Krakow, Poland, September 5-8, 2004, CD Rom.
- [21] Zhao Y, Zou X, Huang D, Liu X, Cao F, Kang Y, "Research on Excitation Control of Flexible Power Conditioner Doubly Fed Induction Machine", *IEEE, Power Electronics Specialists Conference, PESC 2007*, pp. 92-97, 17-21 June 2007.
- [22] Knudsen H, Nielsen J N, "Introduction to the Modelling of Wind Turbine", In *Ackermann T, Editor, Ed., Chichester, U.K: Willey, ("In Wind Power in Power Systems")*, pp.525-85 2005.
- [23] Ogata, K., 'Modern Control Engineering', Prentice Hall, 1970.
- [24] Xie Zhen, Zhang Xing, Yang Shuying, Li Qin and Zhai Wenfeng, "Study on Control Strategy of Maximum Power Capture For DFIG in Wind Turbine System", 2010 2<sup>nd</sup> *IEEE International Symposium on Power Electronics Distributed Generation Systems*, pp.110-115, June 2010.
- [25] Janaka B. Ekanayake, Lee Holdsworth, Xueguang Wu and Nicholas Jenkins "Dynamic Modeling of Doubly fed Induction Generator Wind Turbines", *IEEE Transactions on Power Systems*, Vol.18, No.2, pp.803-809, May 2003.
- [26] Devashish, Amarnath Thakur, "A Comprehensive Review on Wind Energy System for Electric Power Generation: Current Situation and Improved Technologies to Realize Future Development," *International Journal of Renewable Energy Research*, Vol.7, No. 4, pp.1786-1805, 2017.
- [27] Maximiliano Ferrari, "GSC Control Strategy for Harmonic Voltage Elimination of Grid- Connected DFIG Wind Turbine," 2014 *International Conference on Renewable Energy Research and Applications (ICRERA)*, Milwaukee, USA, pp. 185-191, 2014.
- [28] Nguyen Gia Minh Thao, Kenko Uchida, Kentaro Kofuji, Toru Jintsugawa, Chikashi Nakazawa, "A Comprehensive Analysis Study about Harmonic Resonances in Megawatt Grid- Connected Wind Farms", 2014 *International Conference on Renewable Energy Research and Applications (ICRERA)*, Milwaukee, USA, pp. 387-394, 2014.
- [29] E. Hamatwi, I E Davidson, M N Gitau, "Control of multi-Level Voltage Source Converters Integrating a Wind Turbine System into the Grid," 2016 *International Conference on Renewable Energy Research and Applications (ICRERA)*, Birmingham, UK, pp.813-819, 2016.
- [30] M.S.Hamad, K.H. Ahmed, "A Multifunctional Current Source Inverter Control for Wind Turbine Grid Interfacing", 2015 *International Conference on Renewable Energy Research and Applications (ICRERA)*, Palermo, Italy, pp. 1328-1331, 2015.